

## GEOLOGY AND MINERALOGY OF LATE MIOCENE CLAYEY SEDIMENTS IN THE SOUTHEASTERN PART OF THE CENTRAL ANATOLIAN VOLCANIC PROVINCE, TURKEY

ALİ GÜREL<sup>1</sup> AND SELAHATTİN KADIR<sup>2,\*</sup>

<sup>1</sup> Niğde University, Department of Geological Engineering, TR-51200 Niğde, Turkey

<sup>2</sup> Eskişehir Osmangazi University, Department of Geological Engineering, TR-26480 Eskişehir, Turkey

**Abstract**—Late Miocene clayey sediments were deposited in lake-margin and shallow-lake environments of the southeastern Central Anatolian Volcanic Province (CAVP). Yellow to red mudstone, alternating with thin beds of conglomerate and sandstone in the Mustafapaşa Formation, is overlain by altered white Cemilköy ignimbrite. Grain size fines upward in each sequence (conglomerate, sandstone, and mudstone). The occurrence of reddish coloration upward, ripple marks, desiccation cracks, plant rootlets and remnants, and the development of initial-stage paleosols in association with smectite reveal that the area underwent alternating periods of siliciclastic and volcanoclastic sediment supply (wet) and drying. Micromorphologically, the development of spongy smectite in mudstone of the Mustafapaşa Formation and vermiform kaolinite in the Cemilköy ignimbrite on resorbed detrital feldspar and devitrified glass reveals *in situ* precipitation driven by dissolution and precipitation mechanisms. In addition, alteration of these sediments may have resulted in the depletion of soluble alkaline elements, such as Ca, Na, and K, from the ignimbrite downward into the Mustafapaşa Formation. Alternatively, the leaching of these elements — due to the hydrologically open system of the lake environment — may have resulted in the enhancement of Al+Fe/Si-favored precipitation of kaolinite in an acidic environmental condition, namely, of the altered Cemilköy ignimbrite at the top of the profile of the Mustafapaşa Formation, and of smectite in an alkaline setting within lower-level sediments where carbonate minerals were lacking. The coexistence of smectite with accessory illite indicates that illitization occurred via release of K and Al during excess desorption of feldspar. Large Ni and Co values in mudstone samples, and Fe oxidized and partly chloritized pyroxene and hornblende, indicate that the basin was also affected by ophiolite-related supply.

**Key Words**—Central Anatolian Volcanic Province, Grain Size, Hydrologically Open Lake System, Kaolinite, Paleoenvironment, Smectite.

### INTRODUCTION

This study covered ~120 km<sup>2</sup> in the southeast part of the Cappadocia region in central Anatolia (Turkey). The occurrence of a large clay deposit in the Late Miocene Mustafapaşa Formation and altered Cemilköy ignimbrite was first discovered during this work. The Mustafapaşa Formation consists of alternating conglomerate, sandstone, and mudstone, and altered Cemilköy ignimbrite.

The Cappadocian Volcanic Province in central Anatolia has been examined previously for various reasons, such as the relationship between magmatism and tectonism (Toprak, 1998; Dhont *et al.*, 1998; Ocakoğlu, 2004), deposition of volcanic materials (Dirik and Göncüçlü, 1996; Pasquare *et al.*, 1988), geochronological, geochemical, and petrographical studies (Pasquare, 1968; Innocenti *et al.*, 1975; Batum, 1978; Ercan *et al.*, 1990; Temel *et al.*, 1998; Aydar *et al.*, 1994; Le Pennec *et al.*, 1994; Pearce *et al.*, 1990),

and mineralogy and origin of clay minerals in the Pliocene fluvial and lacustrine deposits (Gürel and Kadir, 2006). Prior to the present study, no information was available concerning the clay sedimentology and mineralogy of the Late Miocene units.

Therefore, the aim of this paper was to describe the geology, mineralogy, and geochemistry of the southeastern section of the Central Anatolian Volcanic Province (CAVP) sediments, and to discuss the genesis of the clay deposits and their depositional environment within the Mustafapaşa Formation and altered Cemilköy ignimbrite levels.

### GEOLOGICAL SETTING AND DEPOSITIONAL ENVIRONMENT

#### *Geological setting*

In the southeastern part of the CAVP, the Neogene deposits exhibit a gentle topography with respect to the older rocks. Metamorphic basement is the oldest exposed section and consists of Paleozoic mica schists, marble, and Late Cretaceous ophiolitic rocks (Figure 1). In most places, the Neogene sediments overlie discordantly the metamorphic and ophiolitic basement, which

\* E-mail address of corresponding author:

skadir\_esogu@yahoo.com

DOI: 10.1346/CCMN.2008.0560302

are widely exposed around the Paleogene-Neogene lacustrine sediments and ignimbrite (Pasquare, 1968; Göncüoğlu, 1981) (Figure 4). The Paleogene-Neogene stratigraphy starts with the Yeşilhisar Conglomerate and the Çukurbağ Formation, both of Oligocene age. The deposits of the Mustafapaşa Formation (Late Miocene) overlies the former unit with minor discordance. This unit is overlain by the Late Miocene Cemilköy ignimbrite and the lower Bayramhacılı Formation. Between these two units, the altered Cemilköy ignimbrite developed. The Lower Bayramhacılı Formation is overlain by the

Late Miocene Gördeles ignimbrite. These volcaniclastic units are discordantly overlain by Quaternary white travertine and alluvium.

#### Description of the local stratigraphic section

The clay horizons of the study area and their general (Figure 2) and local (Figure 3) lithostratigraphic characteristics have been examined along the river-cut sections and valley outcrops.

As indicated in Figure 2, the basement of the area consists of metamorphic and ophiolitic rocks. These units

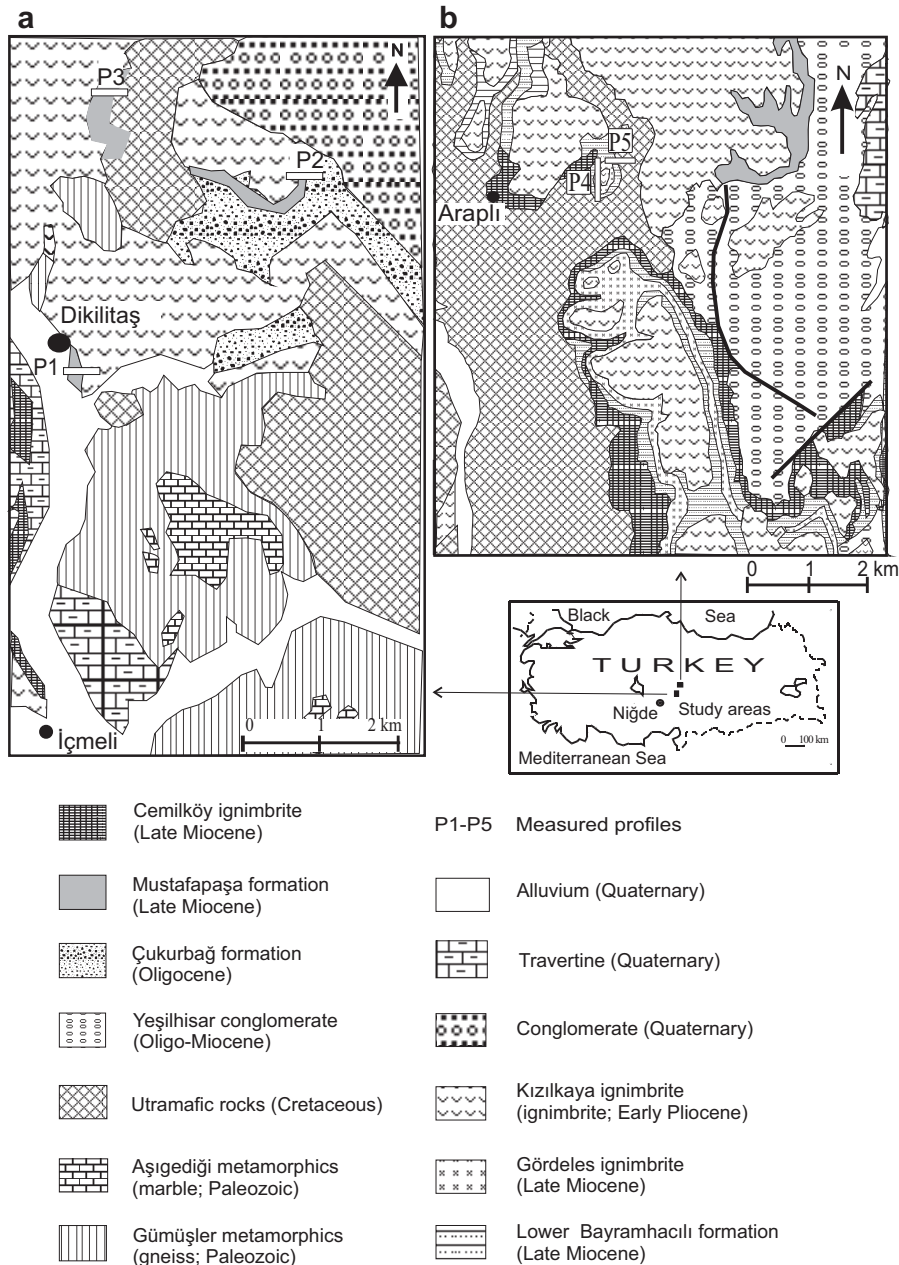


Figure 1. Generalized geological map of the Dikilitaş (a) and Araplı (b) areas (modified from Pasquare, 1968).

are overlain by 18 m thick lacustrine sediments consisting of alternating conglomerate, sandstone, and mudstone, and are known as the Mustafapaşa Formation (Pasquare, 1968). This unit is overlain by the 25 m thick Cemilköy ignimbrite. Well known conical erosion columns (capped earth pillars) are developed within this unit. The abundance of pumice and other clastics increases upward within the formation. The upper level of this unit grades into the altered Cemilköy ignimbrite. This unit then continues upward through the lower Bayramhacılı (20 m), Gördeles ignimbrite (14 m), and upper Bayramhacılı (11 m), respectively, while it also includes two thin fallout levels. The Kızılkaya ignimbrite occurs at the top of the profile reaching up to 20 m thick. Basalt and granite gravels with typical white colors are present in the lower parts of the ignimbrite. Strongly welded reddish ignimbrites occur toward the top of the ignimbritic horizon.

*Lithofacies distribution*

The Late Miocene Dikilitaş-Araplı Plateau is split into southern and northern branches (Figures 3 and 4). A large volume of clay-rich sediments was deposited in the southern branch, which is characteristic of a lake to very shallow lacustrine environment (lake margin), whereas the northern branch is characterized by lacustrine sediments (Pasquare, 1968). Within the Late Miocene sediments of the Dikilitaş-Araplı Plateau, five lithofacies have been distinguished, which are adapted from Miall (1996).

*Massive conglomerate (Gm)*. This facies is represented by gray, massive, unsorted, and subrounded conglomerates. The conglomerate is mainly matrix-supported and may contain <13% matrix. The average clast size is

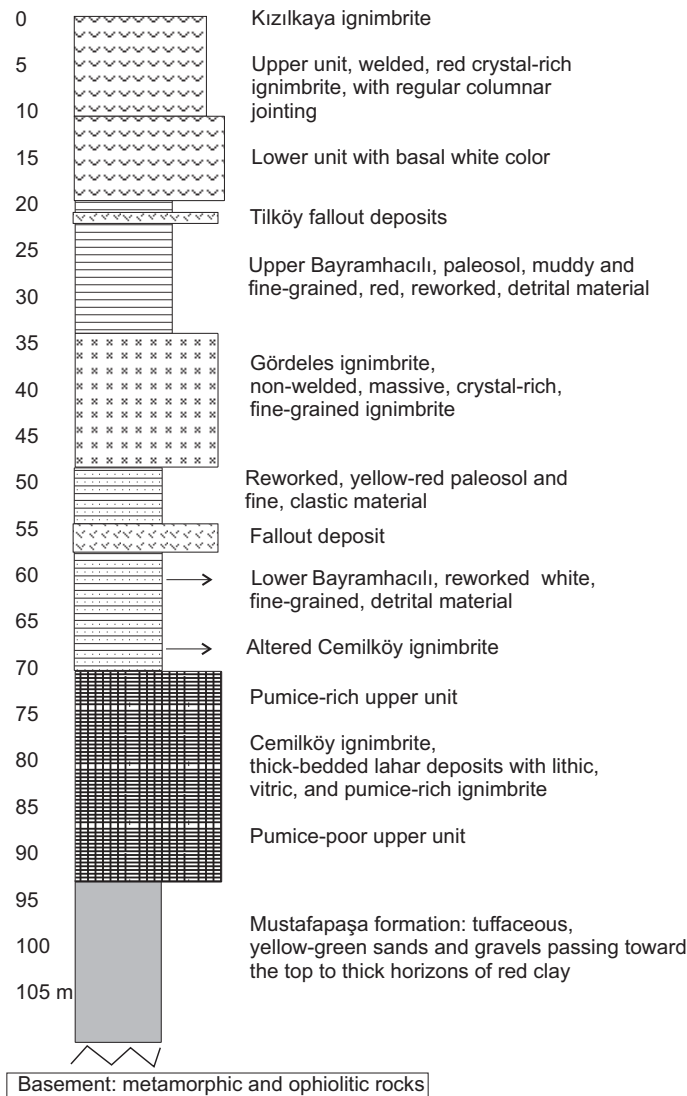


Figure 2. Lithostratigraphic reference profile of the study area.

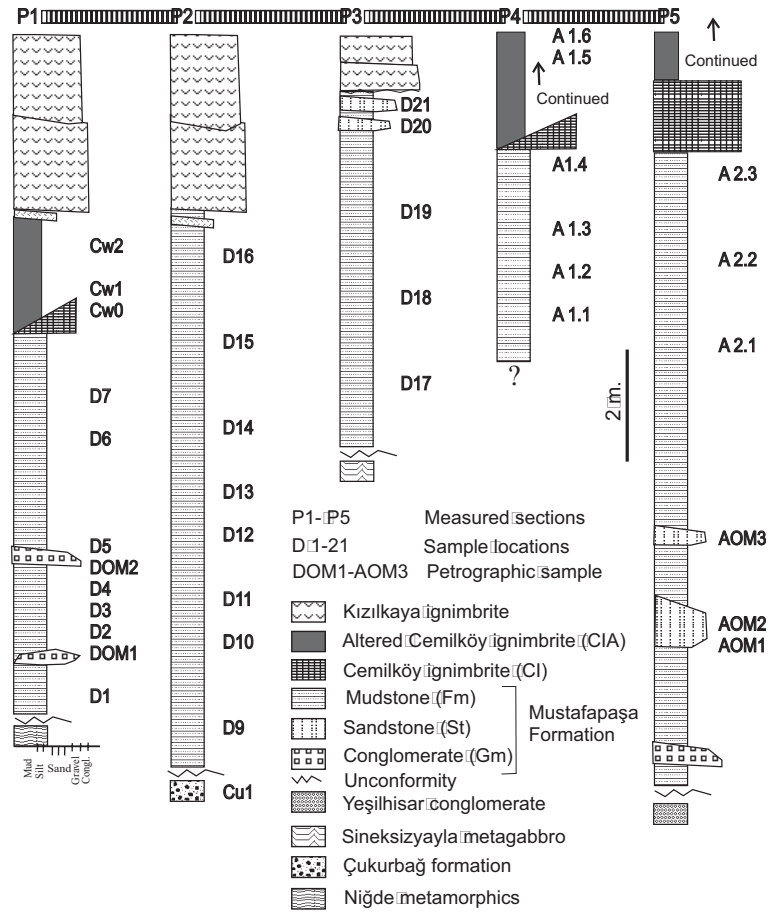


Figure 3. Distribution of the principal lithologies of the southeastern part of CAVP (Dikilitaş-Araplı area).

~20 cm. Measured profiles range between 20 and 40 cm thick. The paleoflow direction is generally south to north. This facies is relatively limited in outcrop.

*Cross-bedded sandstone (St)*. This facies comprises medium to coarse-grained sands and contains rippled, yellow-red, and sharp lower contacts, with plant remnants. Layer thickness varies between 15 and 30 cm. This facies is relatively limited in outcrop.

*Massive mudstone (Fm)*. This facies comprises a yellow-green lower unit with scattered silt particles. These units also enclose plant rootlets and desiccation cracks, a repeating drought environment, and are relatively widespread in outcrop.

*Cemilköy ignimbrite (CI)*. This facies is represented by white, massive, or thick-bedded lahar deposits with lithic, vitric, and pumiceous fragments of ignimbritic origin (Pasquare, 1968).

*The altered Cemilköy ignimbrite (CIA)*. This facies is represented by white, inter-bedded, fine and coarse-

grained tuffs, as well as pumiceous fragments of ignimbritic origin, which exhibit alteration features such as the initial stage of paleosol development. Layer thickness varies between 20 and 50 cm. This facies is relatively limited in outcrop.

#### *Evolution of the Dikilitaş-Araplı plateaux*

Evolution of the plateaux commenced following the diminution or complete cessation of volcanic activity around the Dikilitaş-Araplı area in the Late Miocene. When the lacustrine system had developed completely, two distinct paleogeographic domains with individual characteristics resulted in the lake-margin facies in the southern branch, and lacustrine facies in the northern branch of the study area (Figure 4, Pasquare, 1968).

*Lake-margin sediments (Dikilitaş area; P1–P3, Figures 1a, 2)*. At the end of the Early–Middle Miocene, the areas between Dikilitaş and Araplı developed by tectonic activity, resulting in a narrow and extended lake fed by a longitudinal drainage system. The mudflat units resulted from episodic flood discharges, leading to rapid decantation of clay particles from a

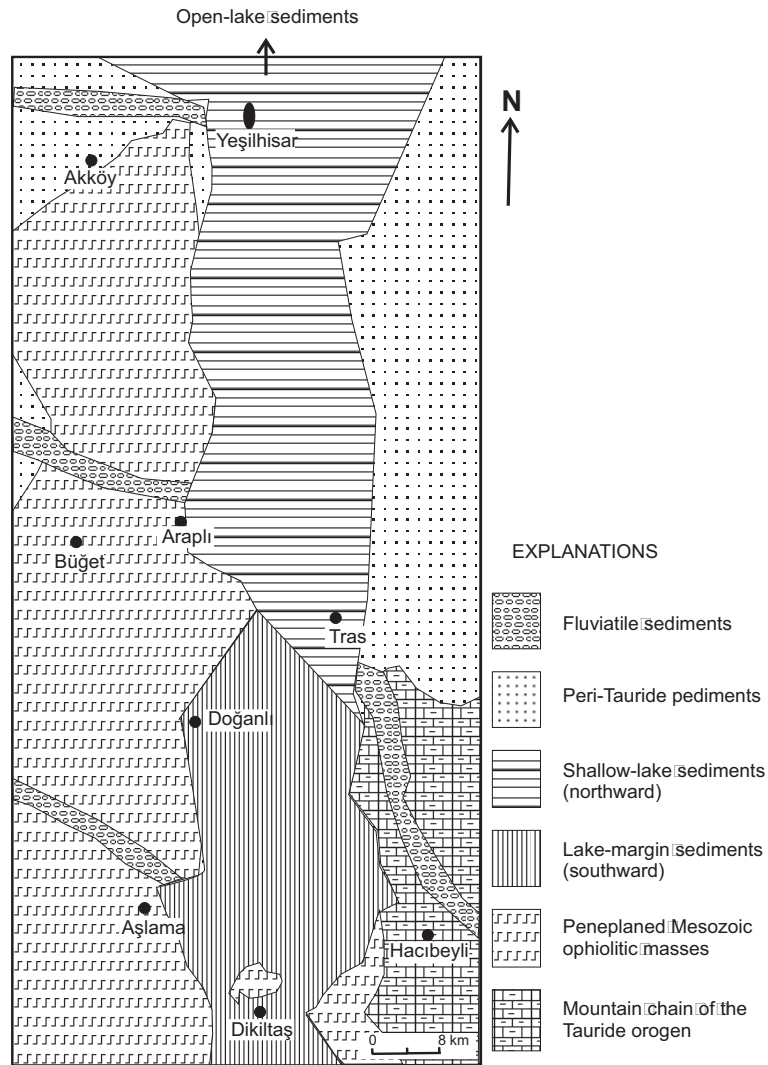


Figure 4. Paleogeographic map of the Late Miocene in the region studied (modified from Pasquare, 1968).

highly concentrated suspension load (Gierlowski-Kodesch, 1998; Aziz *et al.*, 2003). Episodic flood discharges were supported by channel-fill conglomerate and a sandstone structure. These paleoenvironmental conditions during the Late Miocene resulted in the sedimentation of clay particles as red mudstone with thick beds interbedded with thin conglomerate and sandstone which originated mainly from ophiolitic rocks. Each sequence following conglomerate or sandstone is followed by finer-grained materials, which end at the top with the initial development of a paleosol, reddish-brown in color, enclosing root imprints, and desiccation cracks.

*Shallow-lake facies (Araplı area; P4–P5, Figures 1b, 2).* This area, is deeper than the lake-margin facies, and this resulted from decantation of fine material and yellow sediments. The accumulation process is similar to the

reddish mud of the Dikilitaş area, but the yellow coloring suggests that reducing conditions prevailed after deposition in the Araplı area. This indicates that in the Araplı area the lake was shallower due to periodic sediment accumulation and, therefore, the upper levels of the profiles in this area were oxidized and resulted in red coloration similar to that reported by Gürel (2006). The Mustafapaşa Formation sediments in both areas are covered conformably by the Cemilköy ignimbrite and the altered Cemilköy ignimbrite, respectively.

#### MATERIALS AND METHODS

Various river-cut sections and valley outcrops (Figures 1–3) were selected for studying lateral and vertical variations in the sediments. Clay samples were collected from the formations of interest occurring along the Dikilitaş-Araplı plateau and its surrounding areas.

Table 1. The Folk and Ward parameters calculated from the data plotted in Figure 5.

| Folk and Ward parameters  | Conglomerate and sandstone levels | Silty-muddy levels | Altered Cemilköy ignimbrite level |
|---|-----------------------------------|--------------------|-----------------------------------|
| Md $\phi = \phi_{50}$   | 6.20                              | 6.90               | 7.00                              |
| Md = $\phi_{16} + \phi_{50} + \phi_{84}/3$  | 6.00                              | 6.44               | 6.87                              |
| $G\phi = \phi_{84} - \phi_{16}/4 + \phi_{95} - \phi_{5}/6.6$  | 2.07                              | 1.98               | 1.25                              |
| $X\phi = (\phi_{16} + \phi_{84}) - 2(\phi_{50})/2(\phi_{84} - \phi_{16}) + (\phi_{5} + \phi_{95}) - 2(\phi_{50})/2(\phi_{95} - \phi_{5})$ | -0.37                             | -0.99              | -0.45                             |
|   | Coarse-skewed*                    | Coarse-skewed*     | Coarse-skewed*                    |

\* *Sensu* Tucker (1991)

Initially, ~1 kg of samples from each location was taken and air-dried. These samples were investigated by employing the Atterberg method and sieve analysis for the grain-size distribution (Walker, 1971). The grain-size distributions, the median diameter (Md $\phi$ ), the graphical standard deviation ( $G\phi$  = sorting degree), and skewness ( $X\phi$ ), collectively known as the Folk and Ward (1957) parameters, were determined by plotting the data on millimetric paper to draw the cumulative curves.

Representative samples from the various facies were analyzed for their mineralogical characteristics by polarized-light microscopy (Nikon-LV 100Pol), X-ray powder diffractometry (XRD) (Siemens Diffrac-5000 at the Mineralogy Laboratories of Marburg University, Germany), and scanning electron microscopy (SEM-EDX) (JEOL JSM 84A-EDX). The XRD analyses were performed using CuK $\alpha$  radiation and a scanning speed of 1°2 $\theta$ /min. Unoriented mounts of powdered whole-rock samples were scanned to determine the mineralogy of the bulk samples. Samples for clay analysis (<2  $\mu$ m) were prepared by separating the clay fraction by sedimentation, followed by centrifugation of the suspension after overnight dispersion in distilled water. The clay particles were dispersed by ultrasonic vibration for ~15 min. Oriented specimens of the <2  $\mu$ m fraction were prepared from each sample by air-drying, ethylene-glycol solvation at 60°C for 2 h, and thermal treatment at 350°C and 550°C for 2 h. Semi-quantitative measurement of relative rock-forming minerals were obtained by using the external standard method of Brindley (1980), whereas the relative abundance of clay mineral fractions was determined using their basal reflections and the mineral intensity factors of Moore and Reynolds (1989). Representative clay-dominated bulk samples were prepared for SEM-EDX analysis by adhering the fresh broken surface of each rock sample onto an aluminum sample holder, which was covered with double-sided tape and coated with a thin film (350 Å) of gold using a Giko ion coater.

Chemical analysis of representative smectite-, kaolinite-, and illite-bearing samples was performed using inductively coupled plasma atomic emission spectrometry (ICP-AES), for major and trace elements, using inductively coupled plasma mass spectrometry (ICP-MS) for rare-earth elements (*REE*), at Acme Analytical Laboratories, Ltd. (Canada).

The detection limits for analyses were 0.01–0.1 wt.% for major elements, 0.1–5 ppm for trace elements, and 0.01–0.5 ppm for *REE*.

## RESULTS

### Grain-size distribution

Grain-size distribution data were acquired from 21 samples (Figure 5). The results reveal that the Mustafapaşa Formation is a sequence of gravel, sand, and clay levels. The grain-size analyses showed that lower levels of the Mustafapaşa Formation consist of 2.19% gravel, 12.41% sand, 40.03% silt, and 44.66% clay, by weight, whereas the upper levels consist of 12.36% sand, 27.23% silt, and 60.41% clay, by weight. The altered Cemilköy ignimbrite contained ~5.32% sand, 32.20% silt, and 62.48% clay, by weight (larger grains were excluded). Data shown in Table 1 were calculated graphically from the grain-size distributions plotted in Figure 5. The results indicate that the Mustafapaşa Formation and the altered Cemilköy ignimbrite are very poorly sorted and they both show strong positive skewness. Grain-size analyses reveal that clay-sized materials are concentrated mainly in the upper levels of the Mustafapaşa Formation, especially in the altered Cemilköy ignimbrite.

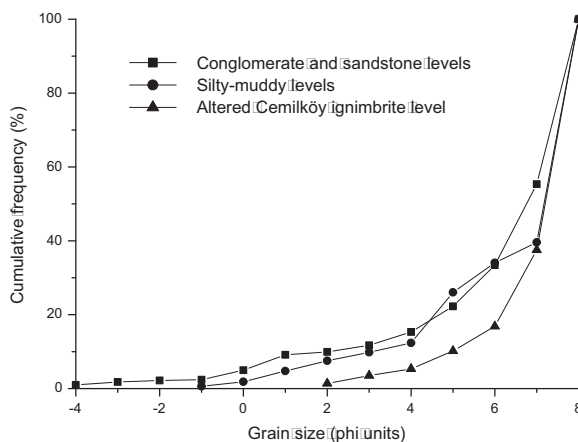


Figure 5. Results of sieve analysis carried out on conglomerate, sand, and silty clay horizons of the Mustafapaşa Formation and the weathered Cemilköy ignimbrite ( $n = 21$ ).

*Mineralogical determinations*

The XRD results for the bulk samples and clayey fraction from the profiles of the studied area are presented in Table 2. Smectite and kaolinite (and illite in samples D16, D20, and D21) are the dominant clay minerals in the southeastern part of the CAVP. Smectite is prevalent in the P1–P5 profiles of the Mustafapaşa Formation, whereas kaolinite increases and smectite

decreases above each profile (Figure 6, Table 2). These minerals are accompanied by feldspar, quartz, opal-CT, biotite, and amphibole. The mineralogical composition and distribution is supported by grain-size distribution and lithofacies descriptions.

Based on the grain-size analyses, clay is abundant in the Mustafapaşa Formation (*e.g.* samples D1 and D2). The XRD analysis of a split representing the clay portion of sample D1, based upon template analysis, indicated

Table 2. Mineralogical variation along stratigraphical sections of the southeastern part of the CAVP (Dikilitaş-Araplı area), Turkey.

|      | smc   | ill | kao   | pal | fds  | qtz | op-ct | hbl | bio | cal |
|------|-------|-----|-------|-----|------|-----|-------|-----|-----|-----|
| P1   |       |     |       |     |      |     |       |     |     |     |
| Cw2  | +     | +   | +++++ |     | ++   | ac  | acc   | acc | +++ |     |
| Cw1  | +     | +   | ++++  |     | +++  | ac  | acc   | acc | ++  |     |
| Cw0  | +++   |     |       |     | ++++ | +++ |       |     |     |     |
| D7   | ++++  | +   |       |     | ++++ | ++  |       | acc |     |     |
| D6   | +++   |     |       |     | +++  | +++ |       | acc |     |     |
| D5   | +++   |     |       |     | +++  | +++ | acc   | acc |     |     |
| D4   | ++++  |     |       |     | ++++ | +++ |       |     |     |     |
| D3   | ++++  |     |       |     | ++++ | +++ |       |     |     |     |
| D2   | +++   |     |       |     | ++++ | +++ | acc   |     |     |     |
| D1   | ++++  |     |       |     | +++  | +++ | acc   |     |     |     |
| P2   |       |     |       |     |      |     |       |     |     |     |
| D16  | +++   | ++  |       |     | +++  | ++  |       |     |     |     |
| D15  | ++    |     |       |     | +++  | +++ |       |     |     |     |
| D14  | ++++  |     |       |     | +++  | +++ |       |     |     |     |
| D13  | +++   |     |       |     | +++  | +++ |       |     |     |     |
| D12  | +++   |     |       |     | +++  | +++ |       |     |     |     |
| D11  | +++++ |     |       |     | +++  | +++ |       |     |     |     |
| D10  | ++++  |     |       |     | ++++ | ++  |       |     |     |     |
| D9   | ++++  |     |       |     | +++  | +   | +     |     |     |     |
| P3   |       |     |       |     |      |     |       |     |     |     |
| D21  |       | +++ |       | +   | ++++ | +++ | acc   |     | +   | +++ |
| D20  |       | ++  |       | +   | ++++ | +++ | acc   |     | +   | +++ |
| D19  | +++++ |     |       |     | +++  | ++  |       |     |     |     |
| D18  | +++++ |     |       |     | +++  | +++ |       |     |     |     |
| D17  | +++++ |     |       |     | ++++ | +++ | acc   |     |     |     |
| P4   |       |     |       |     |      |     |       |     |     |     |
| A1.1 | ++++  |     |       |     | +    | ++  | +     |     |     |     |
| A1.2 | +++++ |     |       |     | +    | ++  | +     |     |     |     |
| A1.3 | +     |     | ++++  |     | acc  | acc | ++    | acc |     |     |
| A1.4 | ++    |     | acc   |     | +    | ++  | +     |     |     |     |
| A1.5 | ++    |     | ++    |     | +    | +   | +     |     |     |     |
| A1.6 | +     |     | +     |     | +    | ++  | +     |     |     |     |
| P5   |       |     |       |     |      |     |       |     |     |     |
| A2.1 | +++++ |     | acc   |     |      |     |       |     |     |     |
| A2.2 | ++++  |     | acc   |     | +    |     |       |     |     |     |
| A2.3 | +     |     | ++    |     | acc  | acc | +     |     |     |     |
| C*   |       |     |       |     | ++++ | acc | acc   | acc | +++ |     |

smc: smectite, ill: illite, kao: kaolinite, pal: palygorskite, fds: feldspar, qtz: quartz, op-ct: opal-CT, hbl: hornblende, bio: biotite, cal: calcite

+: relative abundance of mineral phase, acc: accessory

D1–D21: Dikitaş area, A1.1–A1.4 and A2.1–A2.3: Araplı area (Mustafapaşa Formation)

Cw0–Cw2: Dikitaş area, and A1.5–A1.6: Araplı area (altered Cemilköy ignimbrite)

C\*: The Cemilköy Ignimbrite (Le Pennec *et al.*, 1994), P1–P5: profiles.

The locations of the samples are given in Figure 3.

that abundant smectite is accompanied by a small amount of quartz. Similarly, the altered Cemilköy ignimbrite in the CW0–CW2 samples contains a notable amount of clay, in accordance with the grain-size analysis, and consists of abundant kaolinite, accessory illite, smectite, and trace quartz, based on XRD analysis.

Petrographic examination of the conglomerate reveals the presence of ophiolite-related rocks (gabbro, serpentinite, chert), accessory metamorphic rocks

(gneiss, marble, and mica schist), and sandstone (derived from the Çukurbağ Formation) (Figure 3; DOM1–DOM2). Sandstones of the Dikilitaş and Araplı areas comprise feldspar, pyroxene, ophiolite-related rock fragments, accessory quartz, hornblende, and biotite. Feldspar and pyroxene crystals are generally highly degraded. Most of the pyroxene crystals are heavily Fe oxidized and locally chloritized (Figures 3 and 7; AOM1–AOM3).

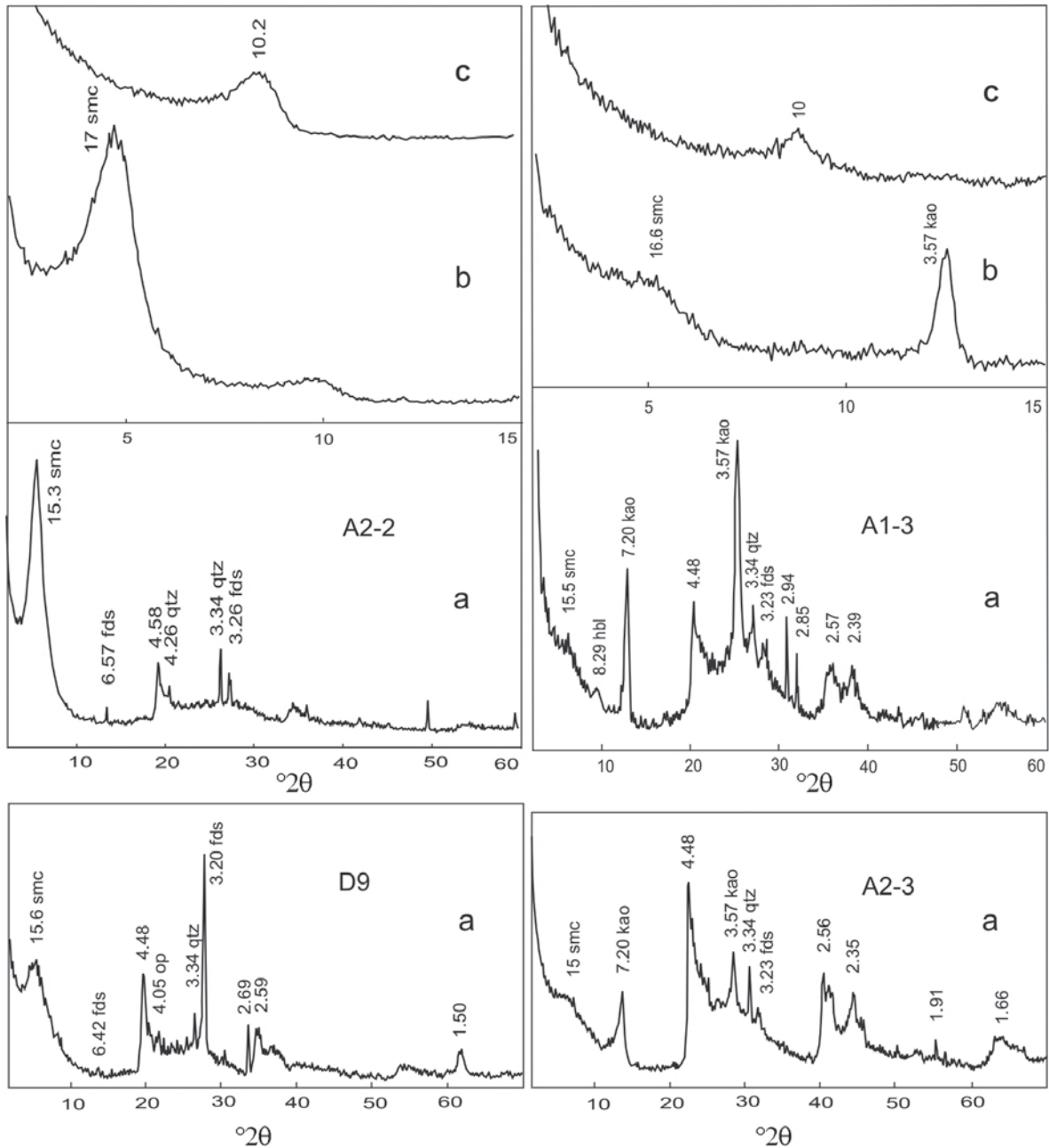


Figure 6. XRD patterns of clay fractions from the Dikilitaş and Araplı areas: (a) powder; (b) oriented; (c) ethylene-glycol solvated; (d) heated to 550°C. smc: smectite; kao: kaolinite; pg: plagioclase; qtz: quartz; op: opal-CT; hbl: hornblende; fds: feldspar.

Well crystallized smectite is distinguished by a sharp peak between 14.43 and 15.8 Å, which expands to ~17 Å with ethylene-glycol treatment and collapses to 9.9 Å after heating at 550°C for 2 h (Figure 6). The  $d_{060}$  value of smectite is 1.49 Å, suggesting a dioctahedral character (Moore and Reynolds, 1989).

Kaolinite was recognized at 7.20 and 3.57 Å, and the 7.20 Å peak was not affected by ethylene-glycol treatment, but did decrease and then collapse upon heating at 350 and 550°C, respectively (Figure 6). Plagioclase was distinguished by diagnostic reflections between 3.18 and 3.22 Å, opal-CT by reflections at 4.05 and 4.10 Å, and hornblende by reflections at 8.2 and 3.12 Å (Figure 6). An increase in the XRD background in most of the samples of the Cemilköy ignimbrite and altered Cemilköy ignimbrite might indicate the presence of opal-A, as reported elsewhere (Jones and Segnit, 1971; Iijima, 1980; Iijima and Tada, 1981).

**SEM determinations.** Siliciclastic and volcanoclastic sediments such as mudstone exhibit desiccation cracks filled by smectite and illite-type, secondary minerals (Figure 8a). Volcanic glass is highly devitrified and

resulted in either a vesicular or degradation character (Figure 8b–g). Relict, degraded glass shards are covered by spongy materials representing smectite, and bar-like structures resembling rhizolite. On the other hand, feldspar crystals are highly resorbed in places (Figure 8h–i). Relict feldspar is surrounded by spongy and cornflake-type smectite. Kaolinite occurs as vermiform crystals ~10 µm in diameter, developed on devitrified volcanic glass (Figure 8j).

Chlorite occurs in a rosette-like form, ~5–8 µm in diameter, developed as a blanket on devitrified volcanic glass along desiccation cracks (Figure 8k–l). Chlorite was determined by optical microscopy, but not by XRD analysis, possibly because its concentration was below the detection limit.

**Geochemistry.** Representative chemical analyses of the samples D1–D4 of the Mustafapaşa Formation, Cw1 (altered Cemilköy ignimbrite) in the Dikilitaş area, A1.2 (Mustafapaşa Formation), and A1.5 (altered Cemilköy ignimbrite) in the Araplı area, are given in Table 3. These units are represented by large values for  $Al_2O_3$

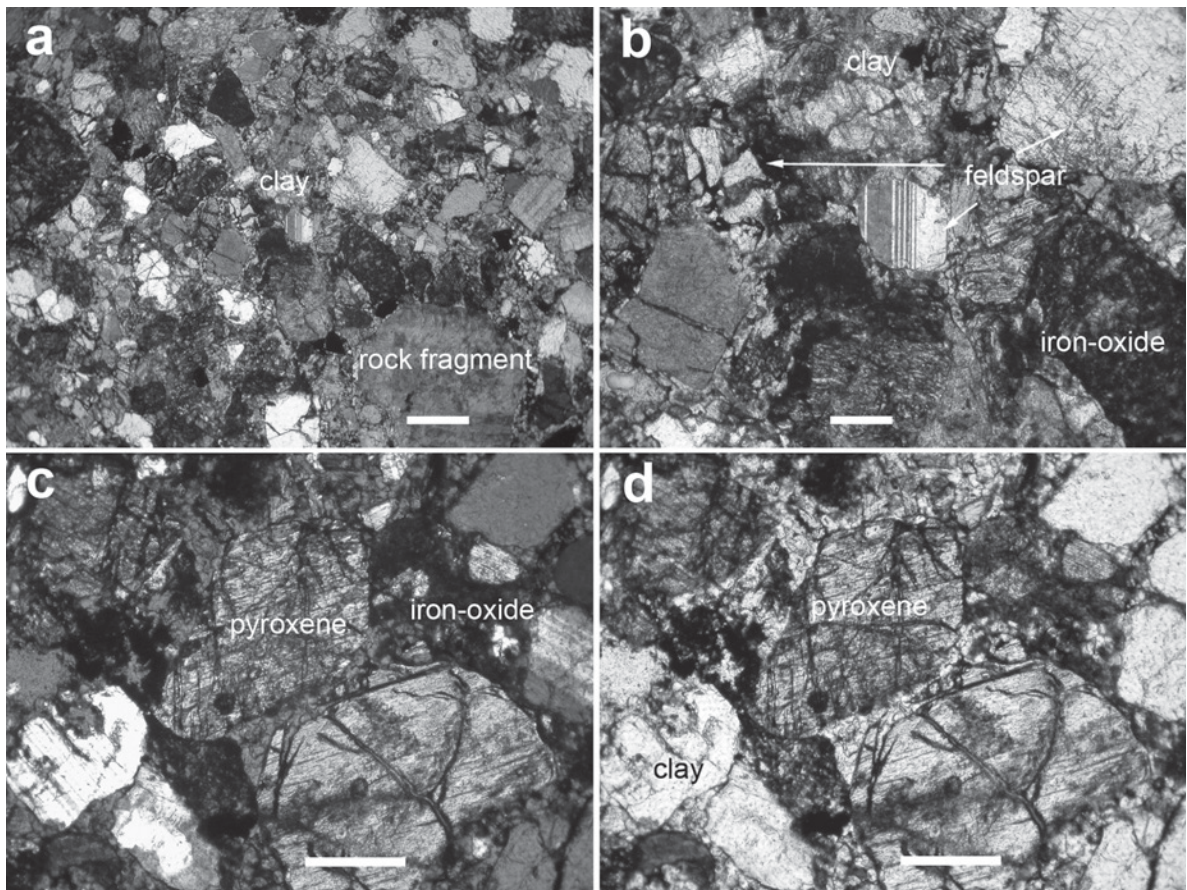


Figure 7. Photomicrographs of: (a–b) volcanic and ophiolite-related minerals and fragments cemented by alteration products and Fe oxide (AOM3, plane-polarized light), scale bar = 5 mm; (c) Fe oxidized and chloritized pyroxene (AOM1, crossed nicols); (d) same as c (in plane polarized light).

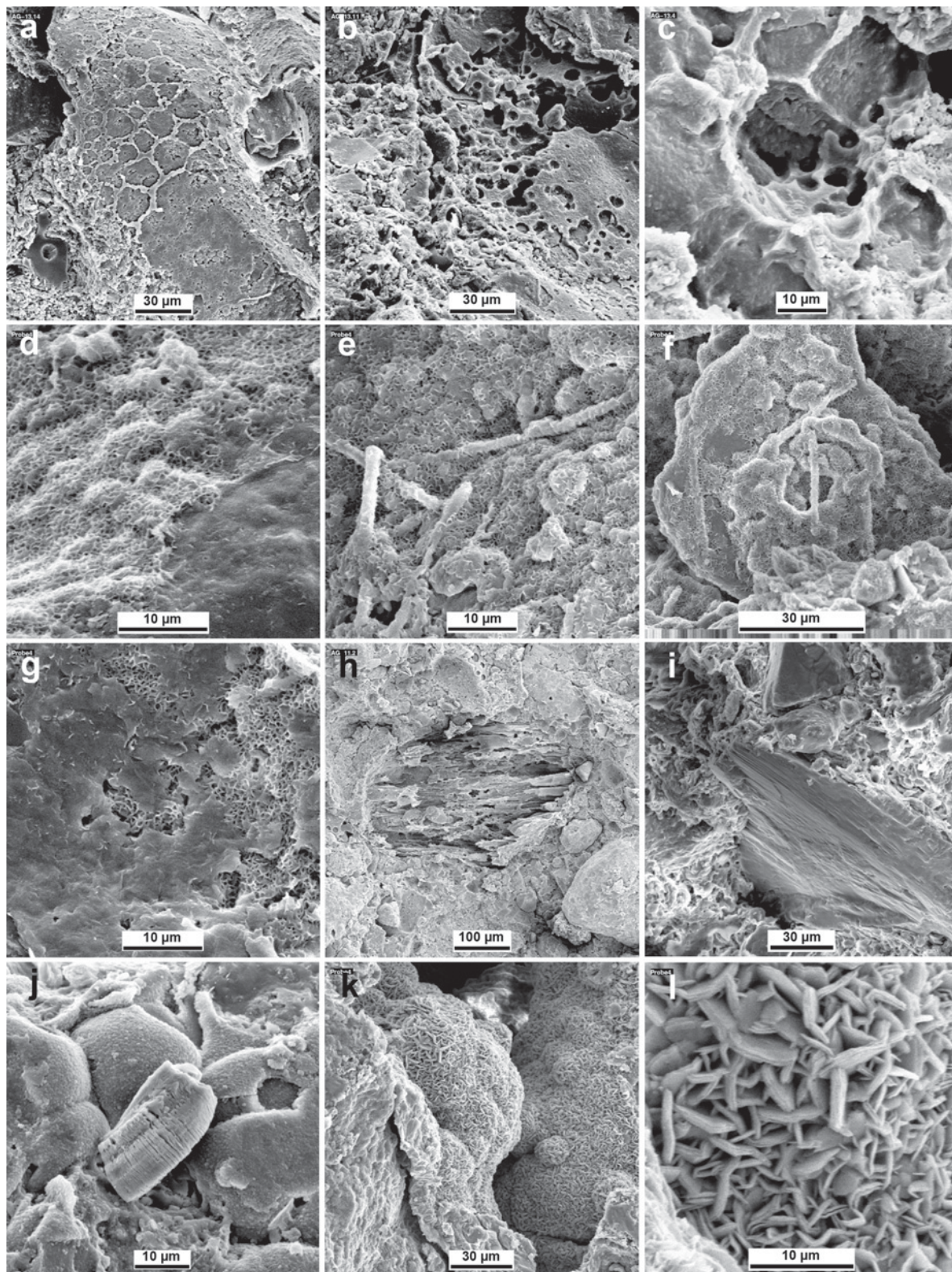


Figure 8. SEM images: (a) desiccation cracks of mudstone filled by secondary minerals (D3); (b–g) devitritified volcanic glass covered by spongy smectite crystals with enclosed rhizolite rod in parts e and f (D1–D6). (h–i) Resorbed feldspar crystals covered or cemented by smectite (D6). (j) Development of vermiform kaolinite on devitritified volcanic glass (Cw1). (k–l) Development of rosette-like chlorite on devitritified volcanic glass (D9).

Table 3. Major and trace element contents of clay samples of the Mustafapaşa Formation, and the altered Cemilköy ignimbrite, representing different lithological levels.

| Oxides (%)                     | D1*   | D2    | D3    | D4    | Cw1*  | A1.2   | A1.4  | A2.3   | Ç.Ign.** | A1.5  | A1.6* | Mudstone <sup>(w)</sup> |
|--------------------------------|-------|-------|-------|-------|-------|--------|-------|--------|----------|-------|-------|-------------------------|
| SiO <sub>2</sub>               | 64.06 | 65.45 | 68.83 | 59.53 | 69.67 | 55.32  | 53.81 | 58.93  | 71.89    | 55.71 | 55.69 | 69.67                   |
| Al <sub>2</sub> O <sub>3</sub> | 12.18 | 11.80 | 11.26 | 13.56 | 14.96 | 13.56  | 13.90 | 12.68  | 12.90    | 16.81 | 16.72 | 14.96                   |
| Fe <sub>2</sub> O <sub>3</sub> | 5.97  | 5.83  | 4.96  | 7.05  | 1.60  | 6.70   | 7.30  | 5.91   | 1.74     | 8.67  | 6.57  | 6.15                    |
| MgO                            | 1.89  | 2.22  | 1.90  | 2.64  | 0.30  | 2.16   | 5.05  | 2.05   | 0.39     | 1.21  | 1.80  | 2.6                     |
| CaO                            | 0.96  | 1.22  | 1.07  | 1.28  | 1.32  | 1.44   | 1.39  | 1.12   | 0.80     | 1.31  | 1.40  | 2.2                     |
| Na <sub>2</sub> O              | 1.63  | 1.63  | 1.78  | 1.03  | 2.25  | 0.67   | 0.80  | 0.87   | 1.72     | 0.69  | 0.34  | 1.6                     |
| K <sub>2</sub> O               | 1.44  | 1.45  | 1.60  | 1.49  | 4.25  | 1.08   | 1.10  | 1.10   | 4.11     | 1.55  | 1.85  | 3.6                     |
| TiO <sub>2</sub>               | 0.58  | 0.59  | 0.56  | 0.63  | 0.33  | 0.57   | 0.59  | 0.59   | 0.17     | 0.70  | 0.82  | 0.75                    |
| P <sub>2</sub> O <sub>5</sub>  | 0.03  | 0.04  | 0.06  | <0.01 | 0.03  | 0.02   | 0.01  | 0.01   | <.01     | 0.05  | 0.04  | 0.16                    |
| MnO                            | 0.03  | 0.16  | 0.10  | 0.15  | 0.01  | 0.07   | 0.04  | 0.02   | 0.06     | 0.04  | 0.04  | 0.09                    |
| Cr <sub>2</sub> O <sub>3</sub> | 0.132 | 0.102 | 0.114 | 0.057 | 0.024 | 0.105  | 0.130 | 0.201  | <.001    | 0.007 | 0.14  | —                       |
| LOI                            | 10.9  | 9.2   | 7.6   | 12.3  | 5.0   | 18.57  | 15.88 | 16.56  | 6.1      | 13.0  | 14.6  | 6.3                     |
| TOT/C                          | 0.04  | 0.04  | 0.05  | 0.01  | 0.03  | 0.07   | 0.09  | 0.05   | 0.01     | 0.04  | 0.03  | —                       |
| TOT/S                          | 0.02  | 0.01  | 0.01  | 0.02  | 0.05  | 0.02   | 0.05  | 0.02   | 0.01     | 0.03  | 0.03  | —                       |
| Sum                            | 99.91 | 99.83 | 99.96 | 99.85 | 99.88 | 100.27 | 99.98 | 100.04 | 100.00   | 99.88 | 99.99 | —                       |
| Trace elements (ppm)           |       |       |       |       |       |        |       |        |          |       |       |                         |
| Ba                             | 316   | 401   | 363   | 320   | 679   | 31011  | 24390 | 19876  | 710      | 442   | 314   | 460                     |
| Cu                             | 42    | 76    | 54    | 60    | 27    | 29     | 27    | 28     | <20      | 37    | 38    | 45                      |
| Zn                             | 41    | 81    | 62    | 76    | 36    | 58     | 68    | 62     | 73       | 107   | 92    | 95                      |
| Ni                             | 150   | 290   | 193   | 283   | < 20  | 497    | 498   | 502    | 38       | 74    | 104   | 68                      |
| Co                             | <20   | 34    | 24    | 31    | < 20  | 40     | 49    | 45     | <20      | < 20  | <20   | 19                      |
| Sr                             | 140   | 138   | 136   | 138   | 149   | 101    | 130   | 120    | 80       | 124   | 141   | —                       |
| Zr                             | 86    | 87    | 115   | 85    | 166   | 77     | 79    | 79     | 73       | 123   | 138   | 160                     |
| Ce                             | 33    | 21    | 32    | 40    | 72    | 36     | 45    | 43     | 35       | 86    | 52    | —                       |
| Y                              | 16    | 22    | 19    | 18    | 16    | 19     | 14    | 15     | 13       | 36    | 23    | —                       |
| Nb                             | <10   | <10   | <10   | <10   | <10   | <10    | <10   | <10    | <10      | <10   | <10   | —                       |
| Sc                             | 13    | 18    | 14    | 20    | <10   | 12     | 21    | 18     | 3        | 17    | 19    | —                       |
| Ta                             | <20   | <20   | <20   | <20   | <20   | <20    | <20   | <10    | < 20     | < 20  | <20   | —                       |

Data sources: \* Kayalı *et al.* (2005), \*\* Lepetit *et al.* (2007), <sup>(w)</sup> Wedepohl (1984)

(11.80–16.81%), Fe<sub>2</sub>O<sub>3</sub> (1.60–8.67%), SiO<sub>2</sub> (54.32–71.89%), and loss on ignition (LOI) (5–17%). Loss on ignition is an important indication of alteration, and it increases with increase in clay mineral content. The amount of Al<sub>2</sub>O<sub>3</sub>+Fe<sub>2</sub>O<sub>3</sub> is less, and of SiO<sub>2</sub>, greater, in the Mustafapaşa Formation samples than in those of the altered Cemilköy ignimbrite samples. These values represent abundant smectite associated with quartz in the Mustafapaşa Formation, and kaolinite in the altered Cemilköy ignimbrite.

The significant enrichment of Al<sub>2</sub>O<sub>3</sub> in the ignimbrite, indicating that Al<sup>3+</sup> should be the principal cation in the octahedral sites of the clay structures, is shown in the Al<sub>2</sub>O<sub>3</sub>–Fe<sub>2</sub>O<sub>3</sub>+TiO<sub>2</sub>–MgO (AFM) ternary diagram (Figure 9). The clay samples plot in the same field as that of the average global mudstone value from Wedepohl (1984). However, the Mustafapaşa Formation clays are enriched with trace elements, such as Cu, in comparison to the average global mudstone values. The presence of Ni and Cr<sub>2</sub>O<sub>5</sub> is due to feeding from ophiolitic basement rocks of the study area. The major difference detected between clays of the Mustafapaşa Formation and the altered Cemilköy

ignimbrite was the abundance of Ni and Cr in the clays. The clay was depleted of those elements and, remarkably, enriched in Ba, Fe<sub>2</sub>O<sub>3</sub>, and TiO<sub>2</sub>.

## DISCUSSION

A paleogeographic map of the CAVP basin and sedimentological features, such as fining of siliciclastic and volcanoclastic sediments from Dikilitaş (lake margin; P1–P3) toward Araplı (shallow-lake facies; P4–P5), suggest erosion in the south and redeposition of sediments toward the depositional center in the north (Figures 1 and 4). The proportion of clayey sediments increases vertically upward as well as southward nearer the source area. Northward decrease of Al<sub>2</sub>O<sub>3</sub>/SiO<sub>2</sub> (and LOI) where fine-grained materials dominated, suggests basinward paleoflow of siliciclastic and volcanoclastic sediments (episodic flood discharges). On the other hand, this ratio increases upward in each profile.

The alternation of conglomerate, sandstone, and mudstone, and the decrease of grain size upward and basinward (Figures 3 and 5), were the result of periodic climatic changes. Wet periods, with material being

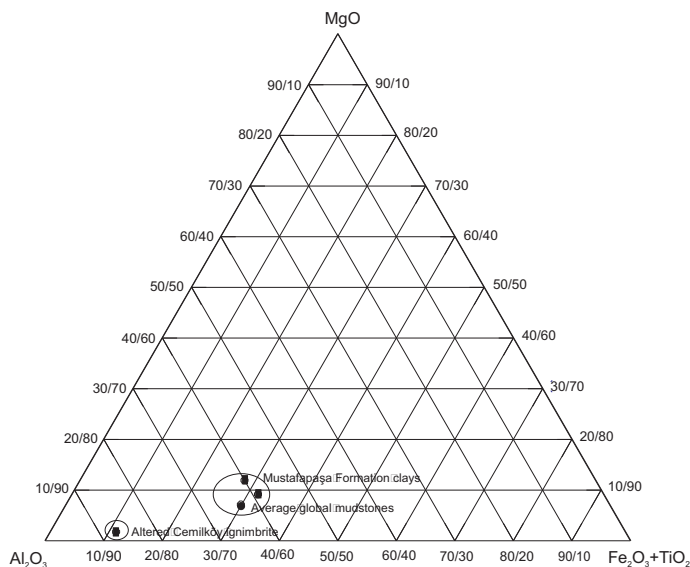


Figure 9. Plot of the average Mustafapaşa Formation clays, the weathered Cemilköy ignimbrite, and the average global mudstone values of the  $\text{MgO-Al}_2\text{O}_3-(\Sigma\text{Fe}_2\text{O}_3 + \text{TiO}_2)$  ternary diagram.

supplied to the basin, favored the formation of smectite via degradation of detrital feldspar, volcanic glass, and ophiolite-related minerals.

The presence of ripple marks, desiccation cracks, plant rootlets and remnants, a sharp lower contact, and a gradual increase of reddish-brown coloration upward in the profiles, in addition to the local occurrence of initial-stage paleosols in association with smectite, reveal that the area was under the control of alternating wet (with siliciclastic and volcanoclastic sediment supply) and dry periods. The reddish coloration is due to relative increase in oxidation (Gürel, 2006). Moreover, weathering might have caused oxidation of structural Fe in smectite to produce changes in color (Komadel *et al.*, 1990; Christidis and Scott, 1997). Thus, these sediments are of alternating yellow and red color in the Araplı area (shallow-lake facies) in contrast to having reddish-brown color in the Dikilitaş area (lake-margin facies). Also, release of Fe, Mg, and Al came about by degradation of pyroxene and hornblende near the source area resulting in Fe oxidation and chloritization, as found through petrographic and SEM determinations. Thus, in the Dikilitaş lake-margin sediments, high Ni (497–502 ppm) and Co (40–49 ppm) values correlate positively with  $\text{MgO}+\text{Fe}_2\text{O}_3$ , indicating either the presence of Fe-Mg-bearing phases, such as pyroxene and hornblende (as determined petrographically), or Ni and Co substitute for Fe and Mg in the octahedral sites of smectite.

The coexistence of smectite with accessory illite in the upper profiles of the Araplı area may indicate that illitization developed by release of K and Al during excess desorption of feldspar, similar to that outlined by Hower *et al.* (1976). Notable enhancement of Ba in the Araplı A1.2, A1.4, and A2.3 shallow-lake mudstone

samples reflects fractional crystallization and concentration by leaching from the upper levels of fresh Ba-rich Cemilköy ignimbrite.

Smectite has been determined to be the main mineralogical component of the Mustafapaşa Formation, in contrast to altered Cemilköy ignimbrite, which is kaolinite-rich. The association of both smectite and kaolinite with detrital feldspar, quartz, and opal-CT, and the development of microscopic spongy and cornflakes-type smectite and vermiform kaolinite on detrital resorbed feldspar and devitrified volcanic glass suggest an authigenic mode of formation for both clay minerals.

The occurrence of two different clay zones, controlled by physicochemical-environmental conditions, has been recognized in the present study. Smectite and kaolinite may have developed *via* the following two processes:

(1) Alteration of feldspar and volcanic glass in altered Cemilköy ignimbrite, in addition to the degradation of ophiolite-related clasts in conglomerate and sandstone of the Mustafapaşa Formation, resulted in the release and depletion of soluble elements, such as Ca, Na, and K, from altered Cemilköy ignimbrite in the uppermost levels downward into the Mustafapaşa Formation and also in an increase of Al and Fe in both altered Cemilköy ignimbrite and the Mustafapaşa Formation.  $\text{Al}_2\text{O}_3$  was enriched in the altered ignimbrite, suggesting that, during the alteration process, mobile elements, such as Na, Ca, and K, were depleted by meteoric and ground water. The overall results were the concentration of  $\text{Al}_2\text{O}_3$  and the precipitation of kaolinite. In contrast, the leaching of alkali elements downward resulted in an alkaline environment appropriate for the precipitation of smectite.

The mobility of these elements during wet periods resulted in an acidic environment appropriate for the precipitation of kaolinite in altered Cemilköy ignimbrite, where the Al+Fe/Si ratio was enhanced (Curtis, 1983; Berner and Berner, 1996; Kadir and Karakaş, 2002; Ziegler, 2006). In contrast, the concentration of alkaline elements and Al+Fe resulted in an alkaline condition suitable for the precipitation of smectite under drought climatic conditions (Grim and Güven, 1978; Weaver, 1989; Chamley, 1989; Christidis *et al.*, 1995). Leaching of silica and concentration of moderately mobile to immobile Al+Fe resulted in a marginward increase of (Al+Fe)/Si in the lake and upward in the profiles. The depletion of excess Si during or after alteration and the precipitation of smectite and kaolinite resulted in the formation of opal-CT.

(2) Under drought conditions, the lake-margin area was fed by rivers and ground water rich in alkaline ions, which originated from extensive weathering of ultramafic rocks. The absence of carbonate and evaporitic minerals might indicate that the lake system was open from the lake margin (Dikilitaş area in the south) toward the lake center (the Araplı area in the north), or even connected to larger lake areas, such as the ancient lake basin of the CAVP (Pasquare, 1968; Figure 4). Dill *et al.* (2005) also described the absence of carbonate minerals in smectite-bearing marginal 'red bed' alluvial-fluvial sediments and the presence of these minerals basin-ward of the Paleogene Ergeliin zoo formation in Mongolia. Depletion of Mg, Ca, and K, and enrichment of Al and Fe+Ti (moderately mobile to immobile elements), resulted in the precipitation of smectite in an alkaline environment (Berner and Berner, 1996). In contrast, in the closed Beypazarı-Çayırhan (central Anatolia) basin, concentrations of Mg, Si, Al, Ca, and Na caused precipitation of sepiolite, loughlinite, palygorskite, smectite, and analcime associated with dolomite, calcite, magnesite, and gypsum in an alkaline environment which developed unconformably on ophiolitic basement rocks, similar to the situations outlined by Echle (1974), Kadir *et al.* (2002), and Karakaş and Kadir (2006). Precipitation of carbonate and evaporite minerals under similar closed environmental conditions in association with clay minerals has been reported in the Pleistocene Lake Tecopa and the Miocene Monterey Formation, the Santa Maria Basin area of California, and the Eocene Pontiles Group, Ebro Basin (Spain) by Starkey and Blackmon (1979), Compton (1991), and Inglès and Anadón (1991), respectively.

The occurrence of calcrete in paleosols and limestones in red Pleistocene sediments of the CAVP (Gürel and Kadir, 2006), in contrast to the carbonate-free red Late Miocene sediments of the Mustafapaşa Formation in the same basin, indicates that sediments of the Mustafapaşa Formation were deposited in a hydrologically open system. Similar individual lakes may pass through hydrologically open and closed phases many

times in their history, such as has been reported for the major East African lakes (Tanganyika, Malawi, Victoria, Albert, Kivu, Turkana, *etc.*) over the last 20,000 y (Street-Perrott and Harrison, 1984; Talbot, 1988; Talbot and Allen, 1996).

## CONCLUSIONS

(1) Late Miocene siliciclastic sediments in the southeastern part of the CAVP were deposited in lake-margin and shallow-lake environments between the present-day Dikilitaş and Araplı areas.

(2) Siliciclastic and volcanoclastic sediments in the Dikilitaş-Araplı area consist of five different lithofacies, namely conglomerate, sandstone, mudstone, the Cemilköy ignimbrite, and altered Cemilköy ignimbrite (profiles P1–P5).

(3) Ophiolitic basement rocks cropped out widely and were progressively eroded and Fe oxidized and chloritized. In this manner, Fe and Mg were supplied to the lake environment, thus contributing to a situation favorable to the formation of clay minerals.

(4) Profiles (P1–P5) enclose two different clay mineral-rich zones: smectite prevailed in mudstone of the Mustafapaşa Formation, controlled by drought conditions, and the occurrence of kaolinite in the altered Cemilköy ignimbrite was controlled by wet climatic conditions.

(5) Smectite increases upward in the profiles and toward the lake margin in the Dikilitaş area, in contrast to the Araplı area where smectite decreases due to episodic flood discharges.

(6) Smectite and kaolinite formed authigenically on resorbed detrital feldspar and volcanic glass shards in the siliciclastic and volcanoclastic sediments.

(7) The Dikilitaş and Araplı areas were characterized by a hydrologically open-lake system during the Late Miocene; thus, carbonate and evaporite minerals are lacking.

## ACKNOWLEDGMENTS

This study was supported financially by the Scientific and Technological Research Council of Turkey (TÜBİTAK) within the framework of Project No. 104Y070. The authors are indebted to Professors Karen Ziegler (University of California), P. Aparicio (University of Sevilla, Spain), Asuman G. Türkmenoğlu (Middle East Technical University, Turkey), and Associate Editors Warren Huff (University of Cincinnati) and Ray E. Ferrell, Jr (Louisiana State University, Baton Rouge, LA) for reviews and suggestions, which improved the quality of the manuscript. We are also grateful to Dr Derek C. Bain (The Macaulay Institute, UK) for his careful editorial comments and constructive suggestions, and to Professor Rudolf Almann (Marburg University, Germany) for his review of an early draft of the manuscript.

## REFERENCES

- Aydar, E., Gündoğdu, N., Bayhan, H., and Gourgau, A. (1994) Volcano – structural and petrological investigation

- of the Cappadocian Quaternary volcanism. *TÜBİTAK Yerbilimleri Dergisi*, **3**, 25–45 (in Turkish with English abstract).
- Aziz, H.A., Sanz-Rubio, E., Calvo, J.P., Hilgen, F.J. and Krijgsman, W. (2003) Palaeoenvironmental reconstruction of a middle Miocene alluvial fan to cyclic shallow lacustrine depositional system in the Calatayud Basin (NE Spain). *Sedimentology*, **50**, 211–236.
- Batum, I. (1978) Geology and petrography of Acıgöl and Göllüdağ volcanics at southwest of Nevşehir Central Anatolia (Turkey). *Yerbilimleri*, **4**, 1–2, 70–88 (in Turkish with English abstract).
- Berner, E.K. and Berner, R.A. (1996) *Global Environment: Water, Air, and Geochemical Cycles*. Prentice Hall, New Jersey, 376 pp.
- Brindley, G.W. (1980) Quantitative X-ray mineral analysis of clays. Pp. 411–438 in: *Crystal Structures of Clay Minerals and their X-ray Identification* (G.W. Brindley and G. Brown, editors). Monograph **5**, Mineralogical Society, London.
- Chamley, H. (1989) *Clay Sedimentology*. Springer Verlag, New York, 623 pp.
- Christidis, G. and Scott, P.W. (1997) The origin and control of colour of white bentonites from the Aegean islands of Milos and Kimolos, Greece. *Mineralium Deposita*, **32**, 271–279.
- Christidis, G., Scott, P.W., and Marcopoulas, T. (1995) Origin of the bentonite deposits of Eastern Milos and Kímalos, Greece: geology, geological, mineralogical and geochemical evidence. *Clays and Clay Minerals*, **43**, 63–77.
- Compton, J.S. (1991) Origin and diagenesis of clay minerals in the Monterey Formation, Santa Maria Basin Area, California. *Clays and Clay Minerals*, **39**, 449–466.
- Curtis, C.D. (1983) Link between aluminium mobility and destruction of secondary porosity. *Bulletin of the American Association of Petroleum Geologists*, **67**, 380–384.
- Dhont, D., Chorowicz, J., Yurur, T., Froger, J.L., Kose, O., and Gündoğdu, N. (1998) Emplacement of volcanic vents and geodynamics of Central Anatolia, Turkey. *Journal of Volcanology and Geothermal Research*, **85**, 33–54.
- Dill, H.G., Kaufhold, S., Khishigsuren, S., and Bulgamaa, J. (2005) Discovery and origin of a Palaeogene smectite-bearing clay deposit in the SE Gobi (Mongolia). *Clay Minerals*, **40**, 351–367.
- Dirik, K. and Göncüoğlu, M. C. (1996) Neotectonic characteristics of central Anatolia. *International Geology Review*, **38**, 807–817.
- Echle, W. (1974) Zur Mineralogie und petrogeneses jungtertiärer tuffitischer Sedimente im Neogen-Becken nördlich Mihalıççık (Westanatolien, Türkei). *Neues Jahrbuch für Mineralogie Abhandlungen*, **133**, 303–321.
- Ercan, T., Fujitani T., Matsuda, J., Tokel, S., Notsu, K., Ul, T., Can, B., Selvi, Y., Yıldırım, T., Fişekçi, A., Ölmez, M., and Akbaşı, A., (1990) The origin and evolution of the Cenezoic volcanism of Hasandağı-Karacadağ area (Central Anatolia). *Jeomorfoloji Dergisi*, **18**, 39–54.
- Folk, R.L. and Ward, W. (1957) Brazos River bar: A study in the significance of grain size parameters. *Journal of Sedimentary Petrology*, **41**, 1045–1058.
- Gierlowski-Kodesch, E. (1998) Carbonate deposition in an ephemeral siliciclastic alluvial system: Jurassic Shuttle Meadow Formation, Newark Supergroup, Hardfort Basin, USA. *Palaeogeography, Palaeoclimatology, Palaeoecology*, **140**, 161–184.
- Grim, R.E. and Güven, N. (1978) *Bentonites, Geology, Mineralogy, Properties and Uses*. Elsevier, Amsterdam, pp. 13–137.
- Göncüoğlu, M.C. (1981) Niğde Masifinde Viridin-Günaysın kökeni. *TJK Bülteni*, **24/1**, 45–51 (in Turkish with English abstract).
- Gürel, A. (2006) Adsorption characteristics of heavy metals in soil zones developed on spilite. *Environmental Geology*, **51**, 333–340.
- Gürel, A. and Kadir, S. (2006) Geology, mineralogy and origin of clay minerals of the Pliocene fluvial lacustrine deposits in the Cappadocian volcanic province, central Anatolia, Turkey. *Clays and Clay Minerals*, **54**, 555–570.
- Hower, J., Eslinger, E.V., Hower, M., and Perry, E.A. (1976) Mechanisms of burial metamorphism of argillite sediments. *Geological Society of America Bulletin*, **87**, 725–737.
- Iijima, A. (1980) Geology of natural zeolites and zeolitic rocks. Pp. 103–118 in: *Proceedings of the 5<sup>th</sup> International Conference on Zeolites* (L.V.C. Rees, editor), London.
- Iijima, A. and Tada, R. (1981) Silica diagenesis of Neogene diatomaceous and volcanoclast sediments in northern Japan. *Sedimentology*, **28**, 185–200.
- Inglès, M. and Anadón, P. (1991) Relationship of clay minerals to depositional environment in the non-marine Eocene Pontils Group, SE Ebro basin (Spain). *Journal of Sedimentary Petrology*, **61**, 926–939.
- Innocenti, F., Mazzuoli, G., Pasquare, F., Radicati Di Brozolo F., and Villari, L. (1975) The Neogene calcalkaline volcanism of Central Anatolia geochronological data on Kayseri-Niğde area. *Geological Magazine*, **112**, 349–360.
- Jones, J.B. and Segnit, E.R. (1971) The nature of opal I. Nomenclature and constituent phases. *Journal of Geological Society of Australia*, **18**, 57–68.
- Kadir, S. and Karakaş, Z. (2002) Mineralogy, chemistry and origin of halloysite, kaolinite and smectite from Miocene ignimbrites, Konya, Turkey. *Neues Jahrbuch für Mineralogie, Abhandlungen*, **177**, 113–132.
- Kadir, S., Baş, H., and Karakaş, Z. (2002) Origin of sepiolite and loughlinitite in a Neogene volcano-sedimentary lacustrine environment, Mihalıççık-Eskişehir, Turkey. *The Canadian Mineralogist*, **40**, 1091–1102.
- Kayalı, R., Gürel, A., Davarçioğlu, B., and Çiftçi, E. (2005) *Investigation of the qualitative and quantitative properties of the raw industrial materials clay and diatomites found in Middle Anatolia by spectroscopic methods*. TÜBİTAK, ÇAYDAG no: 1001Y067, p 157.
- Karakaş, Z. and Kadir, S. (2006) Occurrence and origin of analcime in a Neogene volcano-sedimentary lacustrine environment, Beypazarı-Çayırhan, Ankara, Turkey. *Neues Jahrbuch für Mineralogie Abhandlungen*, **182**, 253–264.
- Komadel, P., Lear, R.P., and Stucki, J.W. (1990) Reduction and reoxidation of nontronite: extent of reduction and reaction rates. *Clays and Clay Minerals*, **38**, 203–208.
- Le Pennec, J.L., Bourdier, J.L., Froger, A., Temel, A., Camus, G., and Gourgaud, A. (1994) Neogene ignimbrites of the Nevşehir Plateau (Central Turkey): stratigraphy, distribution and source constraints. *Journal of Volcanology and Geothermal Research*, **63**, 59–87.
- Lepetit, P., Viereck-Götte, L. and Gürel, A. (2007) Neogene Stratigraphy of the Nevşehir Plateau, Cappadocia, Turkey. Pp. 1–23 in: *Symposium of the Geology of the Cappadocia Region, in the framework of the International Year of Planet Earth* (M. Şener and A. Gürel, editors).
- Miall, A.D. (1996) *The Geology of Fluvial Deposits. Sedimentary Facies, Basin Analysis, and Petroleum Geology*. Springer, Berlin, 582 pp.
- Moore, D.M. and Reynolds, R.C. (1989) *X-ray Diffraction and Identification and Analysis of Clay Minerals*. Oxford University Press, Oxford, UK, 332 pp.
- Ocañoğlu, F. (2004) Mio-Pliocene basin development in the eastern part of the Cappadocian volcanic province (Central Anatolia, Turkey) and its implications for regional tectonics. *International Journal of Earth Science (Geologische Rundschau)*, **93**, 314–328.
- Pasquare, G. (1968) Geology of the Cenozoic volcanic area of

- Central Anatolia. *Atti della Acad. No. delince; memorie serie VIII*, vol. IX s. 55–204, Roma.
- Pasquaré, G., Poli, S., Venzolli, L., and Zanchi, A. (1988) Continental arc volcanism and tectonic setting in Central Anatolia, Turkey. *Tectonophysics*, **146**, 217–230.
- Pearce, J.A., Bender, J.F., De Long, S.E., Kidd, W.S.F., Low, P.J., Güner, Y., Şaroğlu, F., Yılmaz, Y., Moorbath, S., and Mitchell, J.G. (1990) Genesis of collisional volcanism in Eastern Anatolia, Turkey. *Journal of Volcanology and Geothermal Research*, **44**, 189–229.
- Starkey, H.C. and Blackmon, P.D. (1979) Clay mineralogy of Pleistocene Lake Tecopa, Inyo County, California. *USGS Professional Paper*, **1061**, 34 pp.
- Street-Perrott, F.A. and Harrison, S.P. (1984) Lake levels and climate reconstruction. Pp. 291–340 in: *Paleoclimate Analysis and Modeling* (A.D. Hecht, editor). John Wiley, New York.
- Talbot, M.R. (1988) The origins of lacustrine oil source rocks: evidence from the lakes of tropical Africa. Pp. 29–43 in: *Lacustrine Petroleum Source Rocks* (A.J. Fleet, K. Kelts and M.R. Talbot, editors). Special Publication, **40**, Geological Society, London.
- Talbot, M.R. and Allen, P.A. (1996) Lakes. Pp. 83–124 in: *Sedimentary Environments: Processes, Facies and Stratigraphy* (H.G. Reading, editor). Blackwell Science, Oxford, UK.
- Temel, A., Gündoğdu, M.N., Gourgaud, A., and Le Pennec, J.L. (1998) Ignimbrites of Cappadocia Central Anatolia, Turkey: petrology and geochemistry. *Journal of Volcanology and Geothermal Research*, **85**, 447–471.
- Toprak, V. (1998) Vent distribution and its relation to regional tectonics, Cappadocian Volcanics, Turkey. *Journal of Volcanology and Geothermal Research*, **85**, 55–67.
- Tucker, M.E. (1991) *Sedimentary Petrology: An Introduction to the Origin of Sedimentary Rocks*. Blackwell Science, Oxford, UK, 260 pp.
- Walker, R.G. (1971) Nondeltaic depositional environments in the Catskill clastic wedge. *Bulletin of the Geological Society of America*, **82**, 1305–1326.
- Weaver, C.E. (1989) *Clays, Muds, and Shales*. Developments in Sedimentology, **44**, Elsevier, Amsterdam, 819 pp.
- Wedepohl, K.H. (1984) Die Zusammensetzung der oberen Erdkruste und natürlicher Kreislauf ausgewalter Metalle. *Metalle in der Umwelt* (E. Merian, editor). Verlag Chemie, **856**, Weinheim, Germany.
- Ziegler, K. (2006) Clay minerals of the Permian Rotliegend Group in the North Sea and adjacent areas. *Clay Minerals*, **41**, 355–393.

(Received 17 September 2007; revised 28 January 2008; Ms. 0073; A.E. W. Huff)